

Nanonails: A Simple Geometrical Approach to Electrically Tunable Superlyophobic Surfaces

A. Ahuja,[†] J. A. Taylor,[‡] V. Lifton,[§] A. A. Sidorenko,^{||} T. R. Salamon,[†] E. J. Lobaton,[†]
P. Kolodner,[†] and T. N. Krupenkin^{*‡}

Bell Laboratories, Lucent Technologies, Murray Hill, New Jersey 07974

Received July 31, 2007. In Final Form: September 14, 2007

In this work, dynamically tunable, superlyophobic surfaces capable of undergoing a transition from profound superlyophobic behavior to almost complete wetting have been demonstrated for the first time. In the initial state, with no voltage applied, these surfaces exhibit contact angles as high as 150° for a wide variety of liquids with surface tensions ranging from 21.8 mN/m (ethanol) to 72.0 mN/m (water). Upon application of an electrical voltage, a transition from the superlyophobic state to wetting is observed. We have examined experimentally and theoretically the nature of these transitions. The reported results provide novel methods of manipulating liquids on the microscale.

Introduction

It has been known for a long time that a high degree of surface roughness enhances the wetting properties of solids.^{1–4} Modern nanofabrication techniques allow the creation of a wide range of sophisticated surface topographies,^{5–8} such as fractal surfaces,^{7,8} that strongly magnify this effect. Such surfaces serve as a basis for so-called superhydrophilic (water contact angle approaching 0°) and superhydrophobic (water contact angle approaching 180°) materials that demonstrate a range of remarkable properties.^{9,10}

More recently, this approach was extended to demonstrate more advanced types of surfaces that allow dynamic tuning of their wettability all the way from superhydrophobic behavior to almost complete wetting.^{11–14} Although these surfaces show substantial promise for potential applications, their applicability is mostly restricted to high-surface-tension liquids that have a minimum-free-energy state achieved by minimizing the area of contact between the liquid and a solid.^{11,14}

In this work, we propose an approach that allows the creation of a new type of tunable nanostructured surface that operates by

“locking” the liquid in an electrically controllable metastable nonwetting state. This opens up the possibility of creating tunable superlyophobic surfaces (i.e., surfaces capable of demonstrating wetting behavior ranging from complete wetting to active “repelling” of virtually any liquid, independent of its surface tension). The approach relies on 3D nanoscale surface topography, which controllably “pins” the contact line and thus provides a tunable energy barrier capable of holding the liquid in a desirable metastable state. In terms of geometry, this approach further extends the idea of contact line pinning on “mushroom” structures previously proposed in the literature.^{15–17}

Using this approach, we have experimentally demonstrated tunable nanostructured surfaces that are capable of undergoing a transition from profound superlyophobic behavior to strong wetting. In the initial state, with no voltage applied, these surfaces exhibit contact angles as high as 150° for a wide variety of liquids with surface tensions ranging from 21.8 mN/m (ethanol) to 72.0 mN/m (water). Upon application of an electrical voltage, contact angles of the liquids on these surfaces can be reduced to below 30°.

The proposed approach opens a pathway to a simple, material-independent method for creating electrically tunable superlyophobic surfaces and thereby extends many of the potentially attractive properties (high liquid droplet mobility, controllable chemical reaction initiation, tunable drag reduction, etc.^{11–14}) usually associated with tunable superhydrophobic surfaces to a much broader range of materials and applications. To extend previously—demonstrated, dynamically tunable superhydrophobic nanostructured surfaces^{11,14} into the superlyophobic domain, one needs to understand the reasons that prevent traditional superhydrophobic surfaces from being able to “repel” low-surface-tension liquids. When a droplet of a liquid is placed on a very rough surface, such as a fractallike surface^{7,8} or a surface covered with a carpet of high-aspect-ratio micro- or nanoscale spikes, bumps, or posts,^{11,14,18} it assumes a state that minimizes its free energy. This can be achieved by the droplet either wetting the rough surface and thus substantially increasing the total area of the liquid–solid interface or by minimizing the liquid–solid contact area by dewetting most of the surface. In the latter case,

* Corresponding author. E-mail: tnk@engr.wisc.edu.

[†] Lucent Technologies.

[‡] Current address: Department of Mechanical Engineering, University of Wisconsin—Madison, 1513 University Avenue, Madison, Wisconsin 53706.

[§] Current address: mPhase Technologies, 150 Clove Road, Little Falls, New Jersey 07424.

^{||} Current address: Department of Chemistry, University of the Sciences in Philadelphia, South 43rd Street, Philadelphia, Pennsylvania 19104.

(1) Wenzel, R. N. *J. Phys. Colloid Chem.* **1949**, *53*, 1466.

(2) Cassie, A. B. D.; Baxter, S. *Trans. Faraday Soc.* **1944**, *40*, 546.

(3) Callies, M.; Queré, D. *Soft Matter* **2005**, *1*, 55 and references therein.

(4) Barthlott, W.; Neinhuis, C. *Planta* **1997**, *202*, 1.

(5) Seemann, R.; Brinkmann, M.; Kramer, E. J.; Lange, F. F.; Lipowsky, R. *Proc. Natl Acad. Sci. U.S.A.* **2005**, *102*, 1848.

(6) Baldacchini, T.; Carey, J. E.; Zhou, M.; Mazur, E. *Langmuir* **2006**, *22*, 4917.

(7) Shi, F.; Chen, X. X.; Wang, L. Y.; Niu, J.; Yu, J. H.; Wang, Z. Q.; Zhang, X. *Chem. Mater.* **2005**, *17*, 6177.

(8) Onda, T.; Shibuchi, S.; Satoh, N.; Tsujii, K. *Langmuir* **1996**, *12*, 2125.

(9) Martines, E.; Seunarine, K.; Morgan, H.; Gadegaard, N.; Wilkinson, C. D. W.; Riehle, M. O. *Nano Lett.* **2005**, *5*, 2097.

(10) Chen, W.; Fadeev, A. Y.; Hsieh, M. C.; Öner, D.; Youngblood, J.; McCarthy, T. J. *Langmuir* **1999**, *15*, 3395.

(11) Krupenkin, T.; Taylor, J.; Schneider, T.; Yang, S. *Langmuir* **2004**, *20*, 3824.

(12) Sun, T.; Wang, G.; Feng, L.; Liu, B.; Ma, Y.; Jiang, L.; Zhu, D. *Angew. Chem.* **2004**, *43*, 357.

(13) Krupenkin, T.; Taylor, J. A.; Kolodner, P.; Hodes, M. *Bell Labs Tech. J.* **2005**, *10*, 161.

(14) Krupenkin, T. N.; Taylor, J. A.; Wang, E. N.; Kolodner, P.; Hodes, M.; Salamon, T. R. *Langmuir* **2007**, *23*, 9128.

(15) Bico, J.; Thiele, U.; Queré, D. *Colloids Surf., A* **2002**, *206*, 41.

(16) Herminghaus, S. *Europhys. Lett.* **2000**, *52*, 164.

(17) Shirtcliffe, N. J.; McHale, G.; Newton, M. I.; Chabrol, G.; Perry, C. C. *Adv. Mater.* **2005**, *16*, 1929.

(18) Rosario, R.; Gust, D.; Garcia, A. A.; Hayes, M.; Taraci, J. L.; Clement, T.; Dailey, J. W.; Picraux, S. T. *J. Phys. Chem. B* **2004**, *108*, 12640.

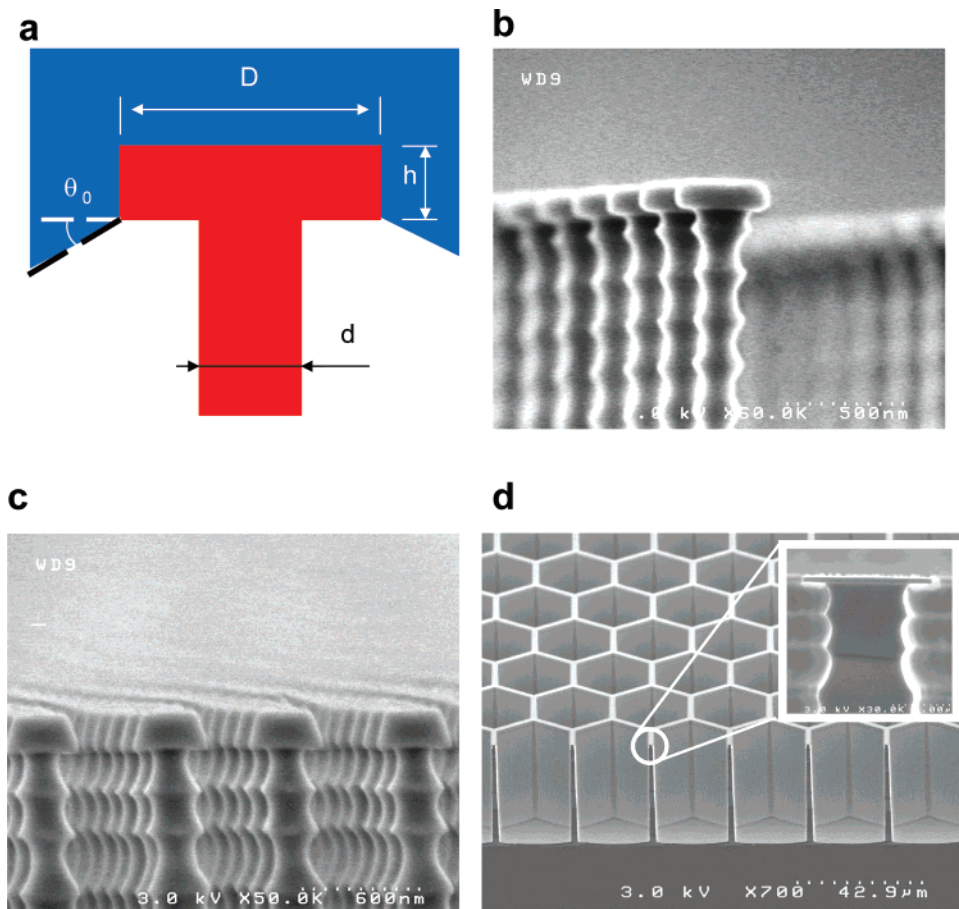


Figure 1. Nanostructured substrate topography. (a) Schematic representation of the overhang geometry. The solid structure is shown in red, and the liquid is shown in blue. (b) Scanning electron microscopy (SEM) image of 2- μm -pitch nanonails. The nail head diameter D is about 405 nm, the nail head thickness h is about 125 nm, and the nanonail stem diameter d is about 280 nm. (c) SEM image of 0.9- μm -pitch nanonails. The nail head diameter D is about 383 nm, the nail head thickness h is about 187 nm, and the nanonail stem diameter d is about 260 nm. (d) Side view of the honeycomb substrate. The cells are arranged on a hexagonal lattice with a period of 30 μm . The inset shows a close-up view of the overhang on the honeycomb wall. The overhang extends approximately 0.4 μm on each side of the wall.

the droplet remains attached to the substrate at a relatively small number of points on top of the structured layer, such as at spike tips or nanopost tops.^{11,14,18} In the first case, the state of the droplet is described by the Wenzel equation,¹ and in the second case, by the Cassie–Baxter equation,² often referred to as the Wenzel and Cassie–Baxter states, respectively.

The Cassie–Baxter state forms the basis of superhydrophobicity. In this state, the liquid–solid contact area and thus the liquid–solid interaction are greatly reduced, and the liquid behaves to a large extent as if supported by a thin air layer rather than by a solid substrate. This behavior leads to a plethora of unusual properties, including extremely high contact angles, high contact-line mobility, and substantial slip at the liquid–substrate interface.^{2–19}

The free energy of a liquid droplet in the Wenzel and Cassie–Baxter states depends strongly on the equilibrium contact angle that the liquid exhibits on the same substrate in its unstructured, flat topographical form. For high-surface-tension liquids with flat-substrate contact angles well above 90° , the Cassie–Baxter state typically provides the minimum-energy state and gives rise to superhydrophobicity. For very low surface tension liquids, according to the Fox and Zisman equation,²¹ the flat-substrate

contact angle goes well below 90° . In this case, the Cassie–Baxter state typically becomes unstable, and the liquid tends to assume the minimum-energy Wenzel state in which the substrate is fully wetted. For a detailed discussion of the conditions under which the transition between Cassie–Baxter and Wenzel states occurs, see ref 15. The behavior described above is observed for all types of superhydrophobic surfaces and prevents them from exhibiting superlyophobic behavior (i.e., being able to “repel” liquids with very low surface tension).

One obvious way to extend the applicability of traditional superhydrophobic surfaces into the superlyophobic regime is to ensure that the Cassie–Baxter state always remains the minimum-free-energy state. This can be achieved by developing coatings with extremely low surface energies so that the flat-substrate contact angles are well above 90° even for low-surface-tension liquids. Some limited success using this approach has been achieved recently, with several researchers reporting self-assembled-monolayer-coated nanostructured surfaces that support contact angles on the order of 120° for a few liquids with moderately low surface tension, such as organic oils.^{6,20,22} However, the applicability of this approach is rather limited. Its further extension to a broader range of important low-surface-tension liquids such as organic solvents and oils that are ubiquitous in the human environment and have surface tensions of around 20 mN/m and below requires the development of stable coatings

(19) Lau, K. K. S.; Bico, J.; Teo, K. B. K.; Chhowalla, M.; Amaratunga, G. A. J.; Milne, W. I.; McKinley, G. H.; Gleason, K. K. *Nano Lett.* **2003**, *3*, 1701.

(20) Tsujii, K.; Yamamoto, T.; Onda, T.; Shibuichi, S. *Angew. Chem., Int. Ed.* **1997**, *36*, 1011.

(21) Fox, H. W.; Zisman, W. A. *J. Colloid Sci.* **1950**, *5*, 514.

(22) Hikita, M.; Tanaka, K.; Nakamura, T.; Kajiyama, T.; Takahara, A. *Langmuir* **2005**, *21*, 7299.

with surface energies of just a few mN/m, well below any values reported in the literature to date.^{10,20,23,24} Moreover, even in its present form, this approach relies on the quality of a delicate, very-low-energy coating, which makes the system highly vulnerable to surface contamination and degradation.

Experimental Results and Discussion

In this work, we propose and experimentally demonstrate a new approach that relies almost exclusively on surface topography to achieve the desired substrate wetting properties. Instead of attempting to guarantee that the Cassie–Baxter state always remains the minimum-energy state, we create a system in which the strength of the energy barrier that separates the metastable Cassie–Baxter state from the stable Wenzel state is designed to be high enough to achieve effective locking of the liquid in the desired nonwetting state. The idea is to create a special type of 3D surface topography that normally inhibits transitions from the Cassie–Baxter state to the Wenzel state but would allow such transitions under the influence of external stimuli, such as electrical fields. A particular example of such topography is the “nanonail” structure shown in Figure 1a–c. Each nanonail consists of a conductive silicon stem and a dielectric silicon oxide nail head. The resulting structure is covered with a thin conformal layer of low-surface-energy fluoropolymer. During electrically induced transitions from the nonwetting to the wetting state, the presence of the conductive nail stem allows one to generate high electrical field values in the immediate vicinity of the liquid–air interface, as will be discussed below.

The reason that nanonails are so effective at preventing spontaneous transitions from the nonwetting Cassie–Baxter state to the wetted Wenzel state becomes obvious as one considers the advancing contact angle θ_0 that the liquid has to exceed in order to wet the bottom part of each nail head, as shown in Figure 1a. To achieve even modest values of θ_0 , well below 90° , the liquid surface would have to deform considerably or “sag” in between neighboring nanonails, leading to a liquid–air interface with curvature on the order of several inverse micrometers; see Figure 1b,c. However, according to the Laplace law,²⁵ such a large curvature is possible only in the presence of high hydrostatic pressure, on the order of 10^4 Pa, which is orders of magnitude greater than the capillary pressure in a macroscopic liquid droplet. Thus, unless high pressure is applied, the liquid has to stay on top of the nanonails and is unable to penetrate inside and wet the nanostructured layer. As is evident in Figure 2a,b, the nanonail topography indeed exhibits superlyophobic behavior even for strongly wetting liquids such as ethanol (21.8 mN/m) and methanol (22.5 mN/m), which readily wet a flat fluoropolymer surface and have corresponding contact angles on the order of 40° .

Obviously, the nanonail geometry is not the only structure that allows one to lock the liquid in the nonwetting Cassie–Baxter state. Essentially any geometry that features “overhang” analogues to a nail head would produce similar results. An example of an alternative geometry—honeycombs with overhang—is shown in Figure 1d. The behavior of liquids on this topography is quite similar to the case of nanonail-covered substrates and will be discussed below.

In this work, we experimentally investigated two types of nanonail-covered substrates (Figure 1b,c) and one type of

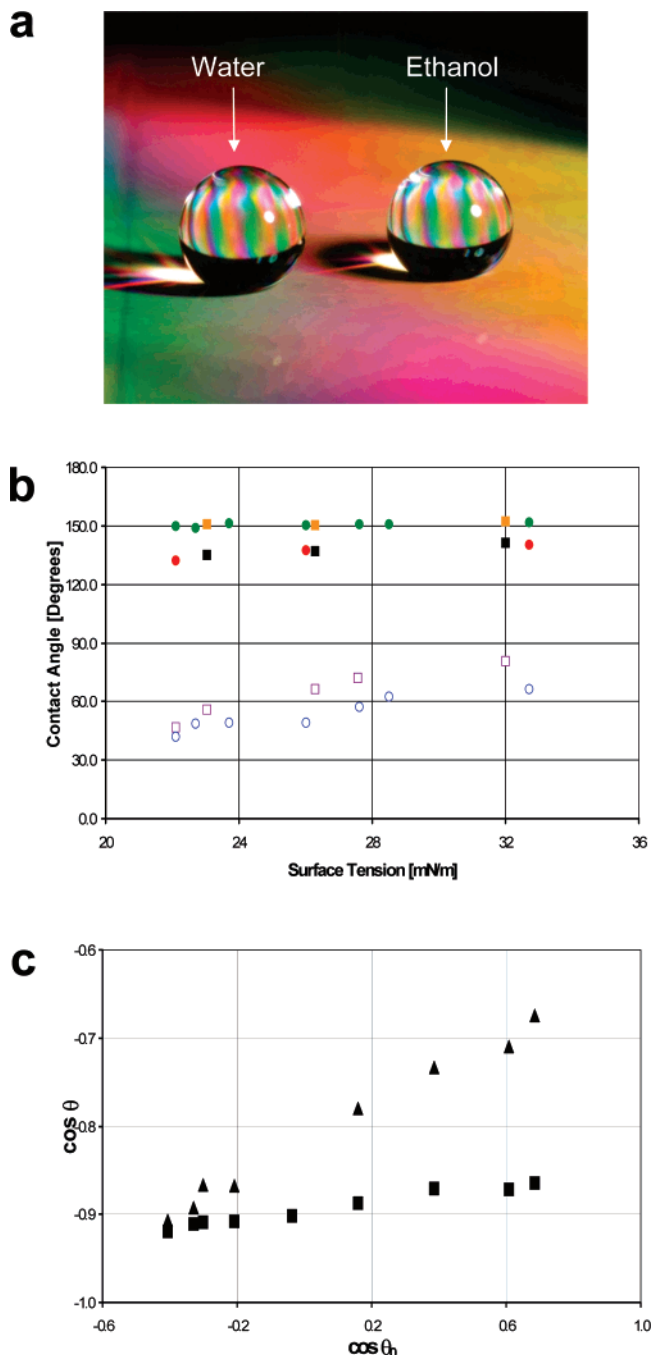


Figure 2. Contact angles of various liquids on nanonail-covered substrates. (a) A nanonail-covered substrate in action. Droplets of two liquids with the very different surface tensions, 72 mN/m (water) and 21.8 mN/m (ethanol), sit next to each other on the $2\text{-}\mu\text{m}$ -pitch nanonail substrate. (b) Contact angles on a flat substrate and on a nanonail-covered substrate vs liquid surface tension. Data for alcohols (from ethanol to cyclopentanol) are represented by circles, and data for water–ethanol mixtures (from 100 to 32% ethanol) are represented by squares. Empty squares and empty circles represent flat-substrate contact angles. Black and yellow squares represent water–ethanol mixtures on nanonails with 0.9 and $2\text{-}\mu\text{m}$ pitch, respectively. Red and green circles represent alcohols on nanonails with 0.9 and $2\text{-}\mu\text{m}$ pitch, respectively. (c) Contact angle cosines on a nanonail-covered substrate vs contact angle cosines on a flat substrate. Squares and triangles represent water–ethanol mixtures (ranging from pure ethanol to pure water) on nanonails with 2 and $0.9\text{-}\mu\text{m}$ pitch, respectively.

honeycomb with an overhang (Figure 1d). The structures were etched in silicon using reactive-ion etching.²⁸ In the case of honeycombs, a layer of thermal oxide approximately 50 nm thick

(23) Bain, C. D.; Evall, J.; Whitesides, G. M. *J. Am. Chem. Soc.* **1989**, *111*, 7155.

(24) Vezenov, D. V.; Zhuk, A. V.; Whitesides, G. M.; Lieber, C. M. *J. Am. Chem. Soc.* **2002**, *124*, 10578.

(25) Adamson, A. W.; Gast, A. P., Eds. *Physical Chemistry of Surfaces*, 6th ed.; Wiley: New York, 1997.

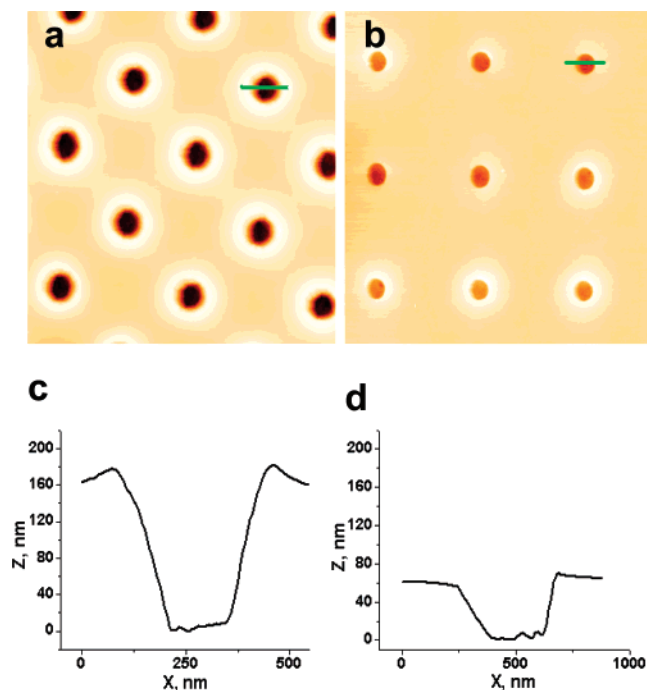


Figure 3. Atomic force microscopy (AFM) images of the solidified liquid-substrate interface. (a) Liquid-substrate interface on a 0.9- μm -pitch nanonail substrate. Color intensity represents surface topography, with the darker colors corresponding to lower elevations. The green line indicates the surface profile scan shown in panel c. (b) Liquid-substrate interface on a 2- μm -pitch nanonail substrate. The green line indicates the surface profile scan shown in panel d. (c) Surface scan through a single nail head imprint shown by the green line in panel a, 0.9- μm -pitch nanonail substrate. The apparent slope of the imprint walls is due to the shape of the AFM scanning tip. (d) Surface scan through a single nail head imprint shown by the green line in panel b, a 2- μm -pitch nanonail substrate.

was grown on the structures using a thermal oxidation process. In all three cases, the structures were conformally coated with an ~ 20 -nm-thick smooth layer of a fluoropolymer^{11,13,14} (F/C ratio of 1.55 and about 18 mN/m critical surface tension) using a chemical vapor deposition process.²⁸ An identical coating was also deposited on flat silicon wafers to allow a comparison with flat-substrate contact-angle measurements. Nanonails with a height of 7 μm were arranged on a square lattice with a pitch of 2 μm , and honeycombs were arranged on a hexagonal lattice with a period of 30 μm . Specific measurements of the nail head and honeycomb geometries are given in Figure 1b–d. A detailed description of the method used to manufacture the structures is available in Supporting Information.

A wide range of low-surface-tension liquids having different chemical natures were used to characterize the superhydrophobic behavior of the nanostructured substrates. Among those tested were alcohols (methanol, ethanol, 1-propanol, 1-butanol, 1-octanol, 1-decanol, and cyclopentanol), water-alcohol mixtures, aromatic hydrocarbons (*o*-xylene and styrene), ethers (1,4-dioxane and anisole), esters (methyl methacrylate), and silicone oils (polyphenylmethylsiloxane and tetraphenyltetramethyltrisiloxane). All of the above-mentioned liquids formed highly mobile droplets on these surfaces, with associated contact angles exceeding 131°.

(26) Brakke, K. A. *The Motion of a Surface by Its Mean Curvature*; Princeton University Press: Princeton, NJ, 1977.

(27) Sethian, J. E. *Level Set Methods: Evolving Interfaces in Geometry, Fluid Mechanics, Computer Vision and Materials Sciences*; Cambridge University Press: Cambridge, U.K., 1996.

(28) Madou, J. *Fundamentals of Microfabrication*, 2nd ed.; CRC Press: Boca Raton, FL, 2002.

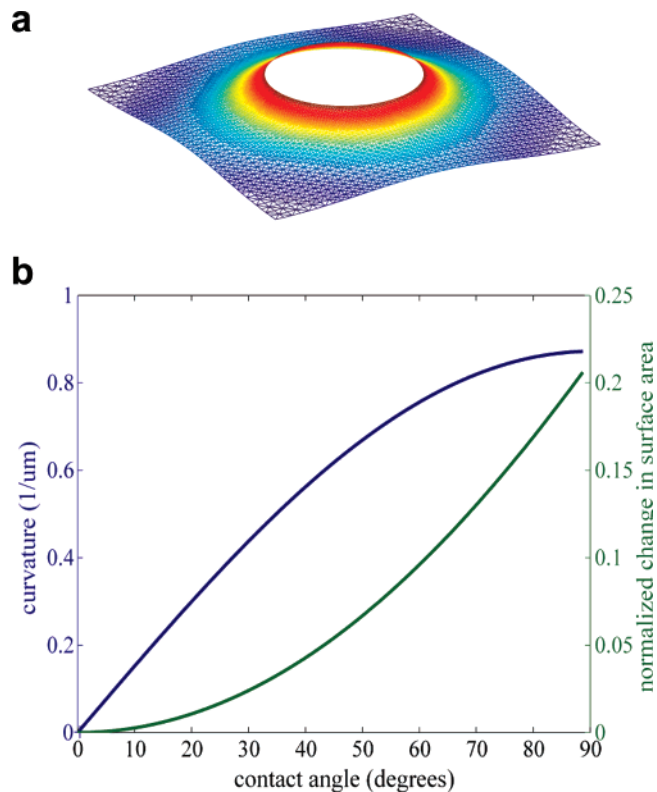


Figure 4. Liquid-air interface modeling results for a 0.9- μm -pitch nanonail substrate. (a) Typical shape of the constant-curvature liquid-air interface. Colors represent surface elevation, with red corresponding to the highest elevation and blue corresponding to the lowest. The hole in the center represents the bottom edge of the nail head. In this example, the interface curvature is equal to 0.55 μm^{-1} . (b) Interface curvature (blue curve) and additional interfacial area with respect to the flat interface (green curve) as a function of the angle θ_0 between the interface and the nail head bottom (Figure 1a).

Typical results for the observed advancing contact angle as a function of the liquid surface tension are shown in Figure 2 using alcohols and water-ethanol mixtures on nanonails as examples. As one can see in Figure 2a, all tested alcohols readily wet flat, fluoropolymer-coated substrates, exhibiting contact angles well below 90°. Yet these liquids form droplets with very high contact angles, approaching 150°, on both 0.9- and 2- μm -pitch nanonail substrates. In addition to demonstrating high contact angles, the droplets on nanonail substrates exhibited very high mobility (i.e., low contact-angle hysteresis), approaching the behavior of “rolling ball” droplets on previously studied nanogras substrates.^{11,14} Water-ethanol mixtures with analogous surface tensions demonstrate similar results and are also shown in Figure 2b. Data for the other liquids on nanonails and the results obtained for honeycombs are available in Supporting Information.

In the Cassie-Baxter state, the cosine of the observed contact angle θ depends linearly on the cosine of the flat-substrate contact angle θ_0 . The experimentally measured dependence of $\cos \theta$ is plotted as a function of $\cos \theta_0$ in Figure 2b for the case of water-ethanol mixtures with surface tensions ranging from pure water (72 mN/m) to pure ethanol (22 mN/m). The observed linear dependence supports our assumption that liquid droplets are in the Cassie-Baxter state on a nanonail substrate.

The position of the liquid-air interface can be directly observed using a polymerization technique.¹¹ In this case, a UV polymerizable monomeric liquid (NOA72, Norland Inc., surface tension 40 mN/m) was employed. After dispensing on the substrate, the NOA72 droplet was polymerized *in situ* by UV irradiation. The solidified droplet was then carefully delaminated

from the substrate, and its bottom surface was investigated using atomic force microscopy (AFM). The AFM results are presented in Figure 3 a–d and show that the liquid–air interface between the posts is substantially flat, as expected from the negligibly small hydrostatic pressure within the droplet. Both the 2 and 0.9- μm -pitch nanonails leave clear imprints along the bottom surface of the droplet, with the imprint depth consistent with the nail head shape as measured from SEM images in Figure 1b,c. Because the nail head shapes are different for the 0.9- and 2- μm -pitch nanonails, the level at which the liquid–air interface resides is also different. For the 2- μm -pitch nail heads, the interface resides approximately halfway between the top and the bottom of the nail head, which is consistent with the $\sim 75^\circ$ flat-substrate contact angle exhibited by NOA72. The conelike shape of the 0.9- μm -pitch nail head precludes the liquid from ever attaining a 75° contact angle with the nail head sidewalls, leading to an interface that is aligned with the bottom of the nail head.

As was discussed above, the shape of the liquid–air interface is determined by the Laplace law, which requires the liquid–air interface to have constant curvature, the value of which is directly proportional to the hydrostatic pressure in the liquid and inversely proportional to the liquid surface tension. The resulting shape of such a constant-curvature interface can be readily calculated using numerical modeling.^{26,27} Typical results of such calculations are shown in Figure 4a. A more detailed discussion of the computational approach can be found in Supporting Information.

Knowledge of the interface shape provides important information about the interface stability because it relates the flat-substrate contact angle to the maximum hydrostatic pressure that the interface can sustain. The transition to the Wenzel state occurs when the liquid–air interface forms an angle with the bottom of the nail head that exceeds the flat-substrate advancing contact angle. In this case, the liquid can advance by wetting the bottom of the nail head and then propagating further down the nanonail. The predicted interfacial curvature is plotted as a function of the local contact angle in Figure 4b. The magnitude of the predicted curvature indicates that even strongly wetting liquids with flat-substrate contact angles as low as $30\text{--}40^\circ$ can sustain substantial pressures on the order of 10^4 Pa. This further supports the notion that the nail heads are capable of strongly inhibiting transitions to the fully wetted Wenzel state.

Similar calculations allow one to estimate a lower bound on the height of the energy barrier that separates the metastable Cassie–Baxter state from the minimum-free-energy Wenzel state. The energy of this barrier is proportional to the liquid surface tension multiplied by the excess liquid–air interfacial area that has to be created to deflect the interface strongly enough to initiate the transition, as discussed above. The results of these calculations are shown in Figure 4b and suggest that the required energy is on the order of 10^{-8} erg, which is orders of magnitude above the characteristic thermal fluctuation energy at room temperature.

A more detailed analysis of the interface stability goes beyond the scope of this letter and will be given elsewhere. Here we simply note that further calculations show that the nail head structures by themselves appear to provide an interface that is rather stable to many common perturbations such as thermal fluctuations, sound, vibration, and so forth. However, the presence of defects such as missing or damaged nanonails, nail heads or delaminated coating or the presence of a hydrophilic particle stuck in between nanonails seem to be capable of substantially reducing the interface stability. Our experimental observations are consistent with this notion.

Switching of the surfaces from the superlyophobic state to the hydrophilic state is achieved by applying a voltage between the liquid and conductive core of the nanonail or honeycomb structure. This procedure is very similar to the one employed to control previously demonstrated tunable superhydrophobic nanostructured surfaces.^{11,14} Because the liquid is electrically isolated from the conductive core of the structures by the silicon oxide overhang, no electrical current develops upon voltage application. However, because of the close spatial proximity, a substantial electrical field can develop in the space between the conductive cores and the liquid. The resulting electrostatic attraction can force the liquid to wet the underside of the overhang, thus inducing a wetting transition. The exact details of this mechanism require further investigation. However, the order of magnitude of the field-induced stress p acting on the liquid–air interface can be estimated by dividing the electrostatic energy stored in the space between the liquid and the tip of each conductive core by their characteristic separation distance s . Assuming that the capacitance of the core–liquid interface scales as $1/s$, we arrive at the following estimate: $p \approx (1/2)\epsilon\epsilon_0 s^{-2} V^2$, where V is the applied voltage, ϵ_0 is the vacuum permittivity, and ϵ is the effective permittivity of the medium in the gap. By substituting characteristic value of separation $s \approx 10^2$ nm and $V \approx 10^1$ V, we obtain $p \approx 10^4$ Pa, which is comparable to the pressure-stability threshold estimated previously from the shape of the liquid–air interface. Thus, at least in principle, direct electrostatic attraction can be sufficient to induce superlyophobic-to-hydrophilic transitions in our structures. The above estimate also indicates that the switching voltage is growing rapidly as the characteristic size of the overhang increases. In particular, it is desirable to have the overhang be a submicrometer size in order to keep the switching voltage within the $10^1\text{--}10^2$ V range.

To investigate electrically induced transitions quantitatively, the apparent contact angle of various liquids was measured as a function of applied voltage. Typical results are shown in Figure 5a–c. As one can see from Figure 5a,b, there is a sharp transition from the superlyophobic state to the hydrophilic state for both nanonail and honeycomb substrates, which is achieved at voltages between approximately 40 and 90 V, depending on the liquid and the substrate. The dependence of the cosine of the contact angle on the square of the applied voltage is shown in Figure 5c using a honeycomb substrate as an example. As expected, liquids with lower surface tension demonstrate smaller contact angles both before and after the transition. Transition voltages, however, do not appear to follow a simple trend. They seem to differ little for butanol, octanol, and cyclopentanol, despite substantial differences in the surface tensions of those liquids. At the same time, the transition voltage for ethanol appears to be substantially higher, despite the fact that it has the lowest surface tension in the group. Additional investigation of the dependence of the transition voltages on the surface tension, hydrostatic pressure, temperature, and chemical nature of the liquids is currently underway and will be published elsewhere.

Conclusions

The dynamically tunable surfaces that were produced require further improvement before they become capable of covering the whole possible range from truly superlyophobic behavior to completely superhydrophilic behavior. However, even in their present form, the exceptional tunability range exhibited by these surfaces makes them unique. We believe that the results demonstrated in this work strongly support the idea of using 3D topography to lock the liquid in a dynamically controllable metastable state. This approach dramatically extends the options

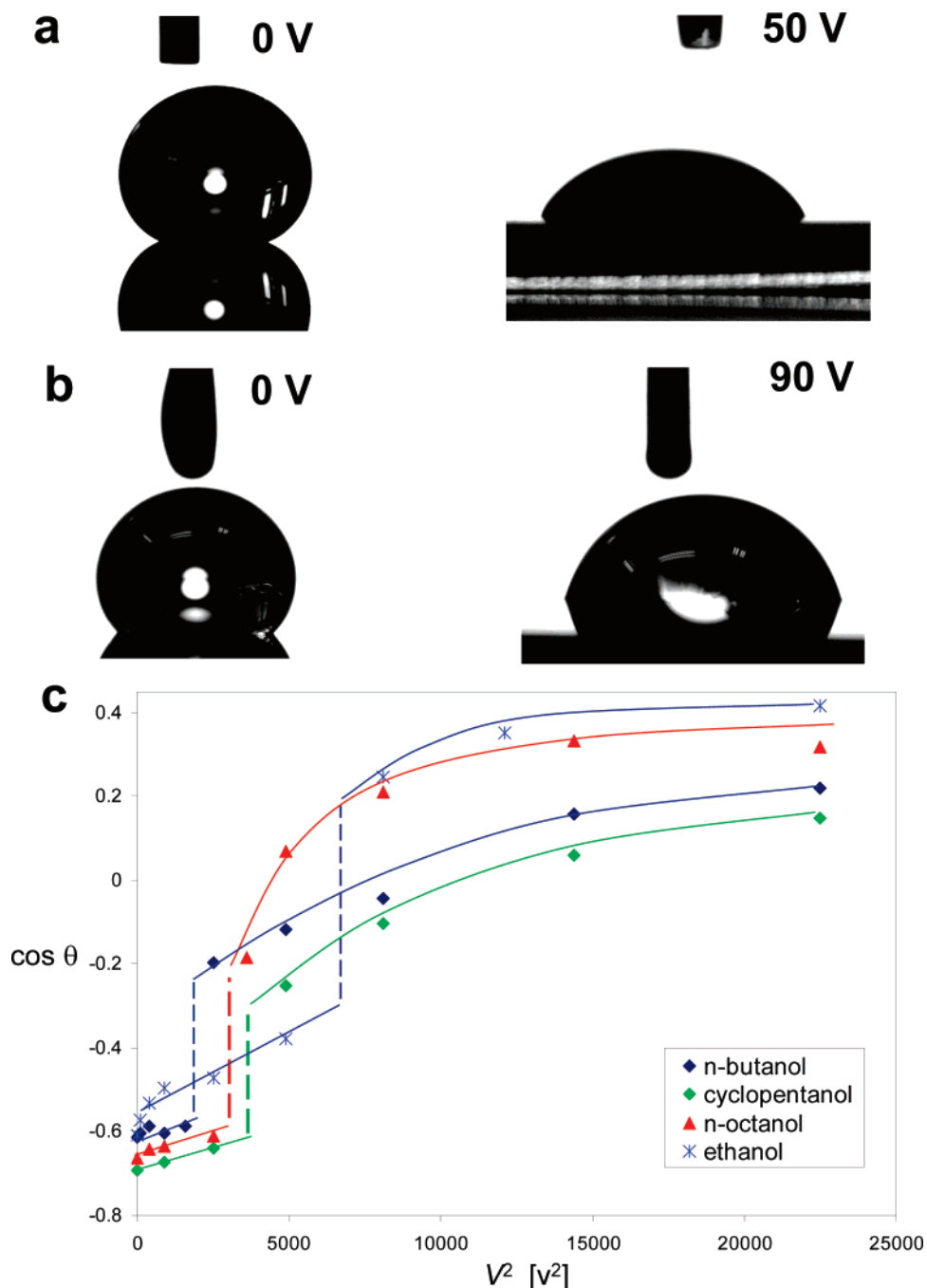


Figure 5. Electrically induced superlyophobic-to-hydrophilic transitions. (a) Droplet of octanol on a $2\text{-}\mu\text{m}$ -pitch nanonail substrate before and after the application of 50 V. The droplet was electrically connected to the voltage source through the syringe needle tip. In the images, the needle is removed to avoid interference with the droplet shape. (b) Droplet of octanol on a honeycomb substrate before and after the application of 90 V. The droplet was electrically connected to the voltage source through the syringe needle tip. In the images, the needle is removed to avoid interference with the droplet shape. (c) Dependence of the cosine of the contact angle θ on the square of the applied voltage V for the honeycomb substrate. Data for four different liquids are shown. Dashed lines indicate the approximate transition voltage, and solid lines are present only to guide the eye.

available to achieving the desired liquid behavior and can open a pathway to the creation of novel materials with new and unexpected wetting behavior. The work presented in this letter is the first to demonstrate tunable superlyophobic surfaces. Droplet-based microfluidics, fluidic drag reduction, lab-on-a-chip devices, and chemical microreactors represent some of the areas that can potentially benefit from such technology.

Acknowledgment. Discussions with Joanna Aizenberg, Mark Hodes, Evelyn Wang, and Mike Bucaro are greatly appreciated. Also appreciated was the processing support from the New Jersey Nanotechnology Consortium.

Supporting Information Available: Materials and methods and numerical modeling. This material is available free of charge via the Internet at <http://pubs.acs.org>.

LA702327Z